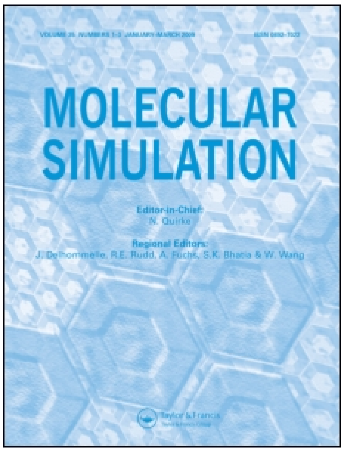

Molecular Simulation
Publication details, including instructions for authors and subscription information:
http://www.informaworld.com/smpp/title~content=t713644482

Sensitivity to guest-host force fields in adsorption equilibrium of cyclic hydrocarbons in one-dimensional molecular sieve

S. M. P. Lucena[a]; J. A. F. R. Pereira[b]; Célio L. Cavalcante Jr.[a]
[a] Dept. Eng. Química, Universidade Federal do Ceará, Fortaleza, CE, Brazil [b] Faculdade de Engenharia Química, Universidade Estadual de Campinas, Campinas, Brazil

To cite this Article Lucena, S. M. P. , Pereira, J. A. F. R. and Cavalcante Jr., Célio L.(2007) 'Sensitivity to guest-host force fields in adsorption equilibrium of cyclic hydrocarbons in one-dimensional molecular sieve', Molecular Simulation, 33: 4, 437 — 448

To link to this Article: DOI: 10.1080/08927020601154280

URL: http://dx.doi.org/10.1080/08927020601154280

Molecular Simulation, Vol. 33, Nos. 4–5, 15–30 April 2007, 437–448

Taylor & Francis
Taylor & Francis Group

Sensitivity to guest–host force fields in adsorption equilibrium of cyclic hydrocarbons in one-dimensional molecular sieve

S. M. P. LUCENA†¶, J. A. F. R. PEREIRA‡§ and CÉLIO L. CAVALCANTE Jr.†*

†Dept. Eng. Química, Universidade Federal do Ceará, Campus do Pici, Bl. 709, 60455-760 Fortaleza, CE, Brazil
‡Faculdade de Engenharia Química, Universidade Estadual de Campinas, Campinas, SP, Brazil

(Received June 2006; in final form November 2006)

We have investigated the effect of different guest–host force fields (united atom, UA; all-atom, AA; and anisotropic united atom, AUA) on the adsorption of cyclic hydrocarbon molecules in $AlPO_4$-5 molecular sieve. Grand canonical Monte Carlo (GCMC) simulations of benzene, xylene and cyclohexane adsorption and positioning are carried out. The results suggest that the force field choice affects considerably the positioning of benzene and cyclohexane molecules while xylenes presented a smaller sensibility. The force fields difference of sensibilities among cyclical molecules seems to be associated with the critical geometric condition identified by Yashonath and Santikary denominated levitation effect. In this condition, the net forces on the guest due to the host is at a minimum, the levitation ratio (γ) is close to unity and we have a weakly bound guest that can be easily moved from its balance position. Unlike xylene, that is only slightly affected by the choice of the force field, benzene and cyclohexane molecules in $AlPO_4$-5 have such dimensions that result in levitation ratio (γ) close to unity. These results point out to the care that should be taken in the choice of the force field when the guest–host size ratio is near the value defined for the levitation effect.

Keywords: Aluminophosphates; Aromatics adsorption; Cyclohexane adsorption; Monte Carlo simulation; Levitation effect

1. Introduction

Molecular simulation has played an important role in the past few years in developing our understanding of the relation between microscopic and macroscopic properties of confined molecular fluids in zeolitic materials [2]. The use of classical potential models has consistently demonstrated their power to describe adsorption of hydrocarbons in zeolites.

All atom or atom–atom (AA) force fields, in which each atom is represented by a separate centre of force, was first proposed by Kiselev and coworkers [3,4] to calculate the thermodynamic adsorption characteristics of hydrocarbons. After that, several authors have proposed united atom (UA) potentials, in which either CH_2 or CH_3 groups are represented by a single centre of force located in the carbon atom [5–7]. The advantage of UA force fields is that they are less time consuming for the calculations than the AA potential models. A third force field approach (AUA, anisotropic united atom) was first proposed by Toxvaerd [8] for *n*-alkanes. Here, the single centre of force is no more located in the carbon atom but displaced towards the geometric centre of the group. The AUA approach is an efficient way to provide more accurate intermolecular potentials without significantly increasing computer time requirements.

Even though cyclic hydrocarbons like aromatics and cycloalkanes are very frequently found in industrial adsorption processes, the number of molecular simulation studies for the adsorption of these sorbates in molecular sieves is still relatively small. More specifically for cycloalkanes, very few studies have been reported. Xylenes in faujasite structures have been studied by several authors [9–12], all of them using AA models for the aromatic ring. Additionally, Lachet and coworkers [11,12] also considered the methyl groups as UAs centred on the carbon. Xylenes adsorption in silicalite was also studied using AA force field in the aromatic ring and UA for the methyl groups [13,14]. We have recently reported studies of xylenes in aluminophosphate molecular sieves

---

*Corresponding author. Email: celio@gpsa.ufc.br
¶Email: lucena@ufc.br
§Email: pereira@desq.feq.unicamp.br

Molecular Simulation
ISSN 0892-7022 print/ISSN 1029-0435 online © 2007 Taylor & Francis
http://www.tandf.co.uk/journals
DOI: 10.1080/08927020601154280

using AA potentials for both aromatic ring and methyl groups [15,16]. For benzene adsorption, all reported studies have used AA force field models for both faujasite [17–19] and silicalite zeolites [13,14,20].

More recently, cyclohexane adsorption in silicalite has been reported with satisfactory results using UA force fields [21–23]. The same UA force field used for silicalite, was also applied to $AlPO_4$-5 [21], showing good agreement for the heats of adsorption values. However, in the latter study, we notice a poor agreement with the experimental results reported by Newalkar *et al.* [24].

From the structural analysis done for the systems of xylenes and aluminophosphates, it was clear that the aluminophosphate pores modulations influence the positioning of the molecules, in such a manner that it may be responsible for the *ortho*-selectivity in those systems [15]. The first objective of the present study is to extend the investigation of this positioning influence to other cyclic molecules as benzene and cyclohexane. Positionings based on experimental data were proposed for benzene and cyclohexane in $AlPO_4$-5 by Chiang *et al.* [25] and Newalkar *et al.* [24], respectively. Chiang *et al.* [25] proposed the face-to-face positioning for benzene while Newalkar *et al.* [24] proposed that the cyclohexane molecules take an upright stance within the channels. In this study, we want to evaluate in more detail, based on molecular simulations, the pores modulations influence for these systems.

The second objective of this study is related to the force field choice, a crucial step in the molecular simulation method. We intend to evaluate the effect of using different force fields available in the literature on the molecule positioning and on the adsorption sites. Besides new AA force fields developed in this study, we will also test UA force fields recently used for cyclohexane [21] and a novel AUA force fields series proposed by Ungerer and co-workers [26–29]. The aluminophosphates one-dimensional channels offer a great perspective for this type of structural analysis because they represent the simplest topology of interconnected pores which are devoid of complications associated with higher dimensional channel systems.

2. Simulation model

2.1 Structural details

The *o*-xylene and benzene molecular structures were considered planar and rigid. We have used the cyclohexane chair conformation in this study, as previously done by Fox *et al.* [21]. Gupta *et al.* [22] have shown that silicalite adsorbs only 2–6% of cyclohexane in the boat conformation.

$AlPO_4$-5 crystallizes in the space group P6/mcc ($a = 13.8$ Å and $c = 8.45$ Å) with 72 atoms/unitary cell [30]. It forms one-dimensional pores with free diameter of 7.3 Å parallel to the crystallographic *c*-direction (AFI structural network—hexagonal).

In aluminophosphates, the channels do not have uniform diameter. They exhibit diameter modulation along the *c*-axis, leading to alternate wide and narrow cross-sections. The narrow region is the ring oxygen windows and the wide region corresponds to the area of connections between two oxygen windows (see figure 1).

$AlPO_4$-5 has narrow windows with 12 oxygen atoms with diameter of 9.96 Å and wide regions (connecting two consecutive windows) with diameter of 11.20 Å.

2.2 Interaction potentials

2.2.1 Sorbate–sorbate interaction. All sorbate–sorbate interactions were modelled with a Lennard–Jones (LJ) potential, with parameters shown in table 1. The cross terms were obtained using arithmetic and geometric combination rules.

The C and H interaction parameters ε_{ij} and σ_{ij} for benzene AA were taken from Jorgensen and Severance [31] that performed Monte Carlo (MC) simulations of pure liquid benzene, benzene in dilute aqueous solution and the benzene dimer in water and chloroform.

The benzene AUA parameters were taken from Contreras-Camacho *et al.* [27]. They have developed a new AUA potential on the basis of the thermodynamic properties of benzene that provide a correct prediction of vaporization enthalpy, vapour pressure and liquid density over a wide range of temperature. We could not find in the literature any studies on benzene adsorption using UA models, so we have not included it for our benzene simulations in our study.

For cyclohexane AA, the parameters came from the "DREIDING" force field [32] used by Kitagawa [10], in a cyclohexane/silicalite energy minimization study. The C and H parameters for cyclohexane UA were taken from Rodriguez *et al.* [33] as previously used by Fox [22]. For cyclohexane AUA, we used the new AUA parameters from Bourasseau *et al.* [29].

In *o*-xylene AA model, C and H parameters were taken from Jorgensen *et al.* [34] which developed an OPLS potential for toluene and other substituted benzenes. An AA model was applied for the substituted benzenes except methyl groups that were treated as UAs centred on the carbon. With the purpose of reproducing a full AA model, we changed the methyl UA for an AA model assigning the carbons in the methyl groups with the same C parameters of the ring carbons atoms.

Figure 1. Cross-sectional and vertical view of the channels of $AlPO_4$-5. There are two diameters in the cross-sectional view, the narrow (9.96 Å) and the broad (11.20 Å). In the vertical view, we can see the different regions indicated along the channel. (Diameters are taken between oxygen atoms of the narrow and wide regions. Aluminum and phosphorus atoms, black balls; oxygen atoms in the windows, gray bars; oxygen atoms in the wide regions, white bars. Cross-sectional views represent one wide and one narrow plane.)

Table 1. LJ potential parameters for benzene, cyclohexane and *o*-xylene.

Interaction	*σ (Å)*	*ε (kcal/mol)*	*δ (Å)*	*Reference*
Benzene AA				
C—C	3.55	0.07	–	Jorgensen and Severance [31]
H—H	2.42	0.03	–	Jorgensen and Severance [31]
C—O	2.99	0.22	–	This study
H—O	2.71	0.068	–	Bhide and Yashonath [35]
Benzene AUA				
CH—CH	3.24	0.177	0.407	Contreras-Camacho *et al.* [27]
CH—O	3.11	0.181	–	Pascual *et al.* [37]
Cyclohexane AA				
C—C	3.47	0.095	–	Mayo *et al.* [32]
H—H	2.84	0.015	–	Mayo *et al.* [32]
C—O	2.99	0.22	–	This study
H—O	2.71	0.068	–	Bhide and Yashonath [35]
Cyclohexane UA				
CH_2—CH_2	3.86	0.102	–	Rodriguez *et al.* [33]
CH_2—O	3.3	0.131	–	Fox *et al.* [21]
Cyclohexane AUA				
CH_2—CH_2	3.46	0.178	0.336	Bourasseau *et al.* [29]
CH_2—O	3.23	0.181	–	Pascual *et al.* [37]
o-xylene AA				
C—C	3.55	0.07	–	Jorgensen *et al.* [34]
H—H	2.42	0.03	–	Jorgensen *et al.* [34]
C3—C3	3.55	0.07	–	This study
C—O	2.99	0.254	–	Bhide and Yashonath [35]
C3—O	3.02	0.185	–	This study
H—O	2.71	0.068	–	Bhide and Yashonath [35]
o-xylene AUA				
CH—CH	3.24	0.177	0.407	Contreras-Camacho *et al.* [28]
C—C	3.06	0.083	–	Contreras-Camacho *et al.* [28]
CH_3—CH_3	3.8	0.17	–	Jorgensen *et al.* [34]
CH—O	3.11	0.181	–	Pascual *et al.* [37]
C—O	3.02	0.124	–	Pascual *et al.* [37]
CH_3—O	3.11	0.395	–	This study

(*) δ is the displacement of the force center for each CH or CH_2 group in the AUA model.

AUA model parameters for *o*-xylene were taken from Contreras-Camacho *et al.* [28]. Since the use of the UA model to represent the methyl groups is very frequently found in xylene simulations, we changed the AUA methyl model for an UA methyl model derived from Jorgensen *et al.* [34].

2.2.2 Sorbate–aluminophosphate interaction. In all systems that were studied, the sorbates were assumed to interact only with the oxygen atoms of the molecular sieve framework. The dispersion–repulsion forces between sorbate and aluminophosphate were modelled using LJ potentials.

The LJ potentials between the hydrogen and oxygen atoms for benzene AA were taken from Bhide and Yashonath [35]. The parameters ε_{ij} and σ_{ij} of the carbon were adjusted so that the value of the benzene–aluminophosphate interaction energy was close to the low loading adsorption heat value observed experimentally for benzene in $AlPO_4$-5 [36].

The benzene AUA CH—O parameters were taken from Pascual *et al.* [37]. In that study, the use of AUA hydrocarbons force field series was extended to adsorption in silicalite. The parameters ε_{ij} and σ_{ij} for the O—O interaction were derived using only experimental equilibrium data for butane adsorption. The O—O parameters thus obtained were $\sigma_O = 3.00$ and $\varepsilon_O = 0.185$. The cross terms between sorbate and molecular sieve were calculated using arithmetic and geometric combination rules. With this method, they could predict adsorption isotherms in a temperature range of 277–374 K for various alkanes in silicalite. In a later study, the same procedure was used to predict hydrocarbons adsorption isotherms in other molecular sieve structures such as TON, FER and BEA with good results [38]. We applied the same procedure to our aluminophosphate molecular sieve.

For cyclohexane AA, we did not find any adsorption simulation study using aluminophosphate fitted AA force fields, so we used the same benzene AA C—O and H—O parameters. The calculated value for the low loading adsorption heat (14.8 kcal/mol) was slightly above the experimentally observed value (13.8 kcal/mol) [24]. For cyclohexane UA, we used the same parameters reported by Fox *et al.* [21]. In that study [21], the same force field that reproduced with success the cyclohexane isotherms in silicalite was used for $AlPO_4$-5. One of our motivations was to confirm the loading values reported by Fox *et al.* [21], a lot above the existing experimental ones. For cyclohexane AUA, we used the same procedure as in benzene AUA.

For *o*-xylene AA, we took the LJ potentials between C and H and the oxygen atoms from Bhide and Yashonath [35]. These parameters were optimized for the system

Table 2. Simulated high loading heats of adsorption in $AlPO_4$-5 (kcal/mol).

Sorbate	*ΔH_{ads} without electrostatic interactions (kcal/mol)*	*ΔH_{ads} with electrostatic interactions (kcal/mol)*	*Difference (%)*
Cyclohexane	15.00	14.80	− 1.3
Benzene	14.8	15.5	4.7
o-Xylene	22.0	19.3	− 12.0

benzene/aluminophosphate. The parameters ε_{ij} and σ_{ij} of the carbon in the methyl group were adjusted in such a way that the xylene–aluminophosphate interaction energy is close to the low loading adsorption heat value observed experimentally for *o*-xylene in $AlPO_4$-5 [25]. Finally, in *o*-xylene AUA, we applied the same methodology used for benzene AUA. Since we were using an UA model to represent the methyl groups, we derived a CH_3—O set of parameters fitted to aluminophosphate. We combined the C—O potential from Bhide and Yashonath [35] with the OPLS CH3—CH3 potential from Jorgensen *et al.* [34] to obtain the methyl UA-oxygen model parameters. The advantage of our approach to obtain new methyl UA-oxygen parameters is that it was optimized for an aluminophosphate molecular sieve [34,35].

As usual, the interactions between Al and P atoms were ignored [4]. The parameters summary for these potentials can also be seen in table 1.

2.2.3 Electrostatic interactions. As previously reported by Clark and Snurr [20], in neutral zeolitic structures, such as silicalite, the contribution of the electrostatic forces in high occupancy adsorption of benzene is only about 5% of the total value of the adsorption heat. Snurr *et al.* [14] have also shown that the electrostatic forces contribution in *o*-xylene/silicalite low occupancy adsorption heat is about 14%. Also, other authors in studies for similar systems [21,35,37] have neglected this contribution. To check the validity of this assumption, we have calculated the high loading heats of adsorption with and without electrostatic interactions (sorbate–sorbate and sorbate–aluminophosphate), as shown in table 2. The long-range electrostatic interactions were evaluated using the Ewald summation method. Karasawa and Goddard [39] discussed extensively the importance of using the Ewald sums method for electrostatic interactions in a molecular sieve periodic system. In this method, the atoms charges are split in two components: one that decays rapidly as a function of a distance (real-space sum) and another component that has small contributions at short distances and is dominated by a long-range term (reciprocal space sum) [40].

The partial charges of the atoms used in this evaluation are listed in table 3 for each sorbate. The charges for *o*-xylene were obtained through semi-empirical calculation (MNDO). The benzene and cyclohexane charges were taken from Snurr *et al.* [14] and Vitale *et al.* [41], respectively. The $AlPO_4$-5 charges were taken from Boutin *et al.* (2.0, 1.6 and − 0.9 $|e|$, for P, Al and O atoms, respectively) [42].

Because of the relatively negligible difference observed for the electrostatic effect in our systems, we decided to proceed with our studies without the electrostatic forces.

2.3 Computational details

The adsorption heats and isotherm calculations were performed in a simulation cell containing 27 unitary cells ($3 \times 3 \times 3$). The GCMC technique was used in the adsorption isotherm simulations [40]. The algorithm allows displacements (translations and rotations), creations and destructions. These simulations consisted of evaluating the average number of adsorbate molecules for which the chemical potential equals that of the bulk phase at a given pressure and temperature.

In the low loading adsorption heat calculations, we used a canonical ensemble MC algorithm (fixed loading) with only four sorbate molecules in the simulation cell, with an initial choice of coordinates for the sorbate molecules, then allowing translations and rotations of the molecules until equilibrium is reached.

The simulations have been performed in a SGI Onyx2 station using Cerius2 software suite [43], which includes the evaluation of the Ewald sums variables (α, the Ewald convergence parameter; r_{cut}, the real space forces cutoff; and $k_{\max}$, the maximum reciprocal lattice vector length that effectively define the range of the reciprocal space sum). Between 1 and 3×10^6 MC steps were performed in order to calculate mean values. The potentials cut off distance was 12 Å, which is of the same order of magnitude of previous studies in similar systems [13,14,44]. The MC algorithms used a bad contact rejection factor (low cutoff) of 0.4 Å. Each run lasted from 1 to 5 h of computing time depending on the simulated system. The UA and AUA models were up to four times quicker than the AA models.

Table 3. Partial charges used in calculating high loading heats of adsorption $|e|$

Atom type	C_{ra}	C_{rb}	C_{met}	H_r	H_{met}	C	H
o-Xylene	0	− 0.12	− 0.159	+ 0.12	+ 0.053	–	–
Benzene†	–	–	–	–	–	− 0.15	+0.15
Cyclohexane‡	–	–	–	–	–	− 0.019	+0.017 (axial) +0.002 (equatorial)

C_{ra}, aromatic ring carbon bonded to methyl radical; C_{rb}, aromatic ring carbon; C_{met}, methyl carbon; H_r, aromatic ring hydrogen; H_{met}, methyl hydrogen.
† From Snurr *et al.* [14].
‡ From Vitale *et al.* [41].

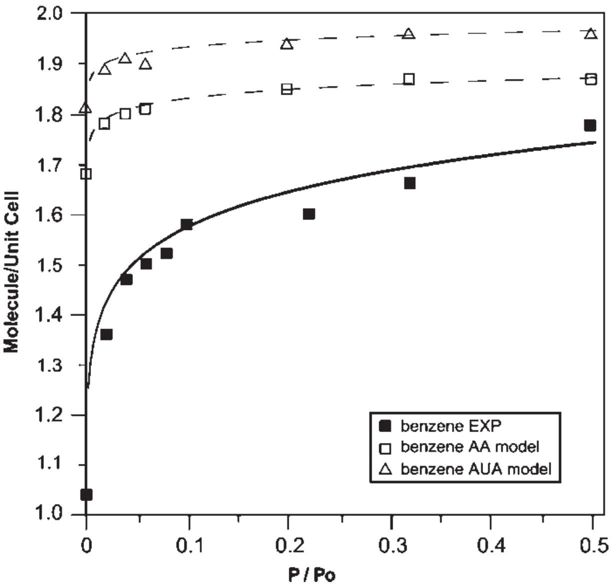

Figure 2. Adsorption isotherms of benzene in $AlPO_4$-5 at 30°C ($P_o = 15.8\,kPa$). Our simulation (dashed lines and open symbols); experimental data [25] (filled lines and symbols).

3. Results and discussions

3.1 Benzene

3.1.1 Adsorption isotherms. The adsorption isotherms of benzene in $AlPO_4$-5 were simulated at 30 °C and compared with experimental data of Chiang *et al.* [25]. Figure 2 presents the simulated and the experimental isotherms. In the experimental isotherm, the adsorbed phase concentration for benzene reaches about 80% of the total sorption capacity still at very low pressures ($P/P_o < 0.03$). The simulated isotherms of both force field models agree well with that characteristic. At the maximum loading ($P/P_o = 0.5$), the AUA force field simulated results show benzene adsorbed phase concentration values about 5% higher than those for the AA force field. Both AUA and AA models yielded adsorbed phase concentrations higher than the experimental reported values at the same loading.

The simulated result for the benzene AA low coverage adsorption heat was very close to the experimental value (13.4 and 13.0 kcal/mol [36], respectively). This was expected, since we have fitted our AA model using the experimental data available. For the benzene AUA model, the simulated low coverage adsorption heat was 12.4 kcal/mol, which is a fairly good approximation since this force field was fitted to butane in silicalite [37].

3.1.2 Structural analysis: molecular positioning and adsorption sites. The structural analysis methodology will be the same as developed in our previous study [15]. The molecular positioning was monitored by the angle between the normal vector of the plane of the benzene ring and the crystallographic *c*-axis. The adsorption sites were determined based in the statistics of centres of mass of the molecules.

We evaluated the angles in the high and low loading regions of benzene adsorption (figures 3 and 4,

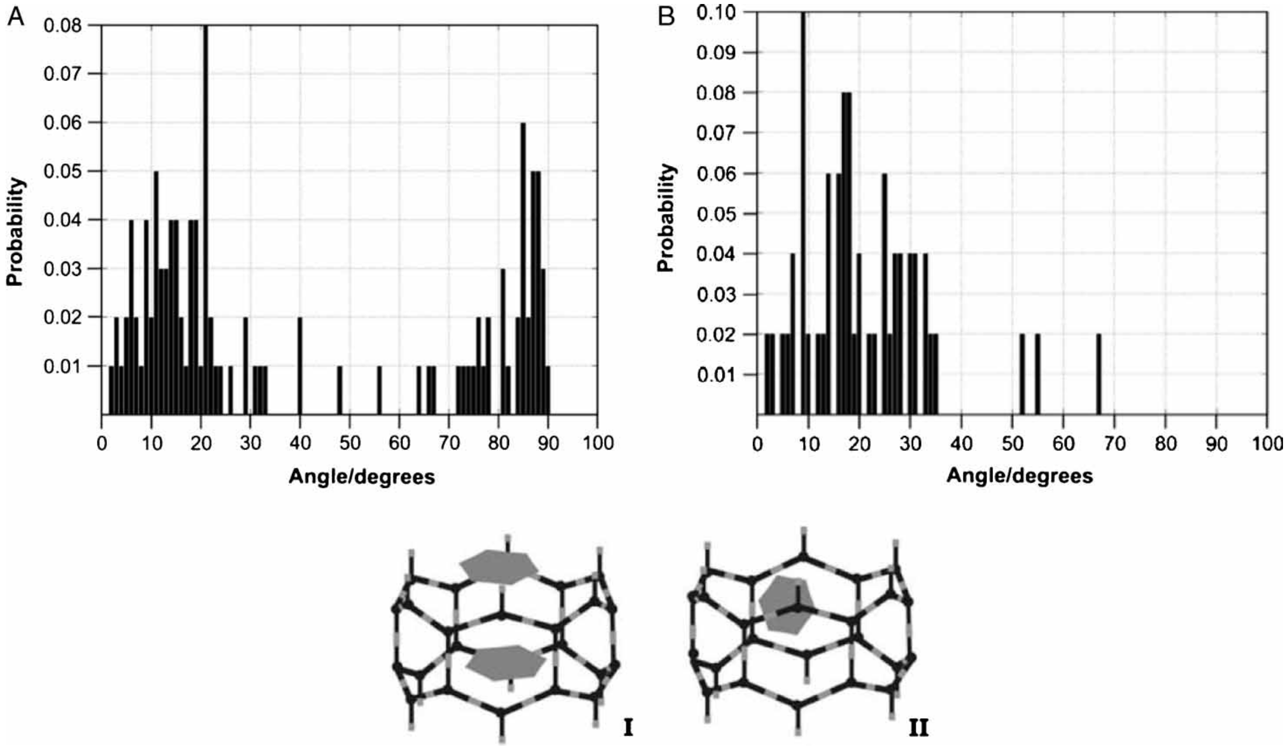

Figure 3. Probabilities for normal angle between the plane of the aromatic ring and the crystallographic *c*-axis at high loading. (A) Benzene AA model. (B) Benzene AUA model. (I) Representation of benzene face-to-face positioning (low angles range in graphs A and B) in the $AlPO_4$-5 wide region. (II) Representation of benzene parallel position (high angles range in graph A) in the $AlPO_4$-5 wide region.

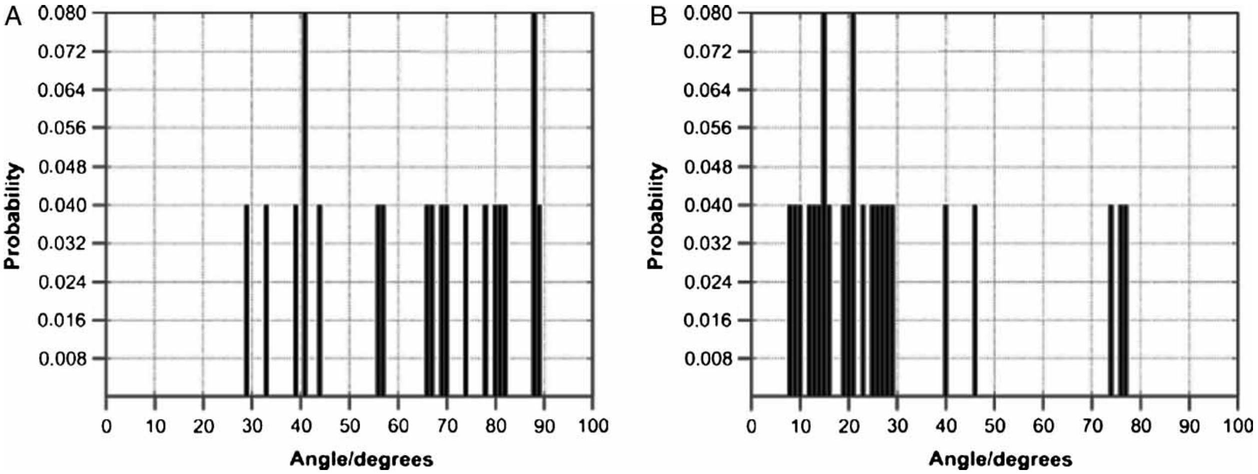

Figure 4. Probabilities for normal angle between the plane of the aromatic ring and the crystallographic *c*-axis at low loading. (A) Benzene AA model. (B) Benzene AUA model.

respectively). For high loading (figure 3), two positionings are dominant: one named face-to-face that corresponds to the range of low angles (from 10 to 20°, see figure 3(A) and graphic representation I) and another named parallel positioning, in the range of higher angles (from 75 to 90°, see figure 3(A) and graphic representation II). For low loading (figure 4), the benzene AA model showed an interesting oscillation between the face-to-face and the parallel positions. When the molecules are in the low density area the parallel position is dominant. Bhide and Yashonath [35], using molecular dynamics, examined the positioning of benzene in $AlPO_4$-5 in the low loading region reaching a similar conclusion. In that study, the angles varied from 65 to 80° along the length of the channels. In our study, the angles are predominant in the 60 to 90° range (figure 4).

In the high loading region, the parallel position is no more predominant and it coexists with the face-to-face positioning. The face-to-face positioning was proposed by Chiang [25] based on experimental data. It seems that the small contribution of the sorbate–sorbate interaction is capable of stabilizing the molecules in the face-to-face positioning when a high loading is achieved. A typical image of the two dominant positions is shown in figure 5.

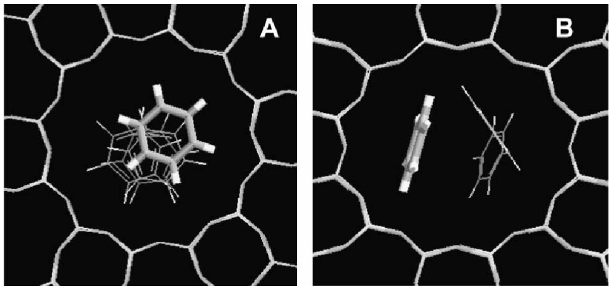

Figure 5. Superior view of the pore with benzene molecules adsorbed in $AlPO_4$-5 at 30°C, showing the suggested dominant patterns. (A) Face-to-face; (B) parallel position.

From figures 3(B) and 4(B), we observe that benzene AUA force field model was not capable to capture this particularity of alteration of positioning. Both at high and low loadings, the face-to-face positioning prevails. Since the parallel positioning slightly decreases the loading, this could be the reason that the AA model yields lower adsorbed phase concentrations than the AUA model, as seen in figure 2.

The mass centres statistics analysis for the benzene AA model (figure 6) indicates that the adsorption sites are located in the wide region of the pores. A similar analysis for the benzene AUA model showed the same results.

3.2 Cyclohexane

3.2.1 Adsorption isotherms. The adsorption isotherms of cyclohexane in $AlPO_4$-5 were simulated in the temperature of 30 °C so they could be compared with experimental data of Newalkar *et al.* [24]. Figure 7 presents the simulated and experimental isotherms.

The values for adsorbed phase concentrations in the simulated cyclohexane AA model are initially larger than the experimental ones, reaching the same value of the experimental data at $P/P_o = 0.5$. A possible explanation is that the real sieve has imperfections so it needs a larger gas phase concentration to reach saturation. In our simulations, the sieve is represented ideally without any imperfections.

The UA and AUA force fields show higher values for the adsorbed phase concentrations (8 and 13%, respectively) when compared to the AA model at the maximum loading ($P/P_o = 0.5$). It is also observed that for all loadings that we studied, both UA and AUA results for the adsorbed phase concentration were higher than the experimental values.

The low coverage adsorption heat calculated for cyclohexane using AA, UA and AUA models were 14.8, 10.0 and 12.5 kcal/mol, respectively. An experimental low coverage adsorption heat was reported as 13.8 kcal/mol [24], showing better agreement for the AA calculated value.

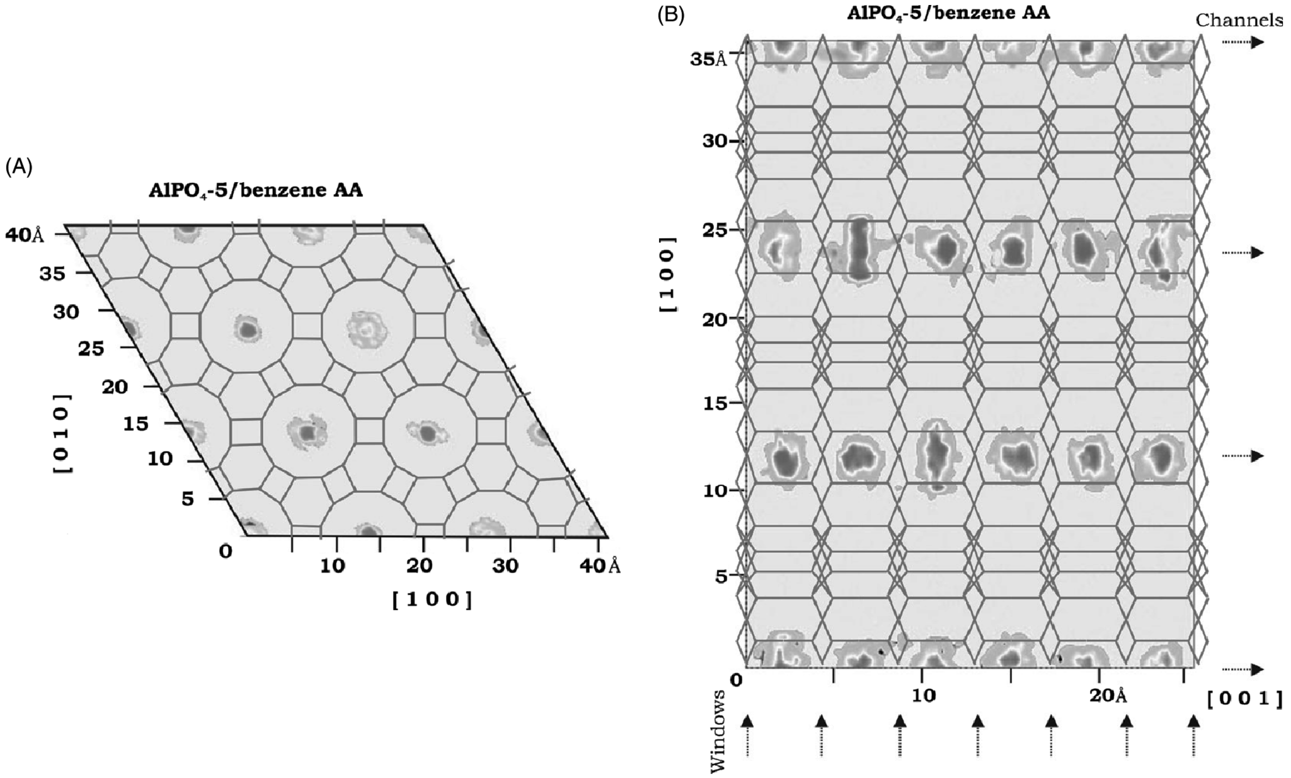

Figure 6. View of the 3 × 3 × 3 simulation cell of $AlPO_4$-5 and benzene with respective statistics of mass centres location of the success moves during simulation for benzene AA model. (A) Projection down plane (0 0 1); (B) projection down plane (0 1 0). Dark areas are of high mass centres occurrence. The benzene AUA model yielded similar results.

3.2.2 Structural analysis: molecular positioning and adsorption sites. Figure 8 shows the angle probabilities for the three models. In this case, we followed the angle formed by the normal vector of the chair conformation of cyclohexane with the crystallographic *c*-axis (figure 8(D)). The most outstanding aspect of these results is that, contrary to what was observed for benzene, cyclohexane does not present a preferential positioning in any of the force fields that were studied. The angles are evenly dispersed for the whole spectrum of possibilities. These results are different to what was proposed by Newalkar *et al.* [24] based on experimental data. According to them, the cyclohexane high packing density is achieved by the molecules adopting an upright stance within the channels. We found that it is not necessary an equivalent upright stance like benzene face-to-face to reach the experimental packing levels, as clearly observed in cyclohexane AA model isotherm results (figure 7). A typical image of the asymmetric molecular pattern of cyclohexane adsorption in $AlPO_4$-5 found in our study is shown in figure 9.

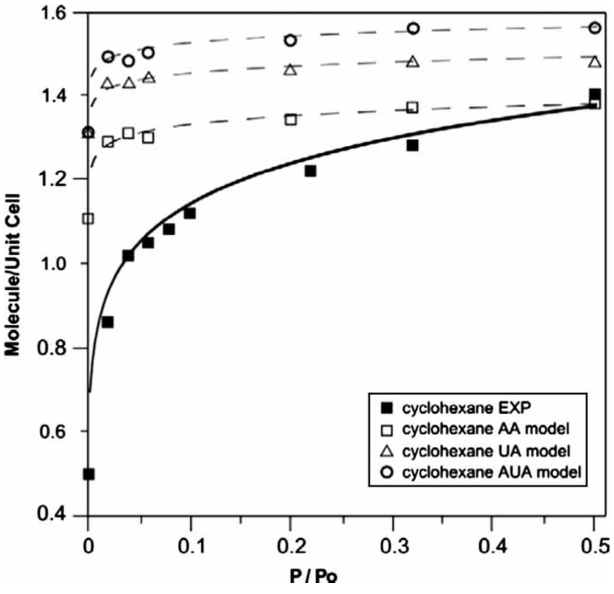

Figure 7. Adsorption isotherms of cyclohexane in $AlPO_4$-5 at 30°C ($P_o = 16.40$ kPa). Our simulation (dashed lines and open symbols); experimental data [24] (filled lines and symbols).

Evidences of the cyclohexane upright stance were reported by Fox *et al.* [21], using the UA model, showing a saturation loading of four molecules per unit cell. In our study, using the same force field parameters, we found an asymmetric pattern for molecules positioning (figure 8(B)) and a maximum loading of only *ca.* 1.5 molecules/unit cell (see figure 7). It is not clear to us the reason for such discrepant results.

The determination of the adsorption sites show large differences among the force fields (figure 10). For cyclohexane AA model, the molecules are preferentially adsorbed in the wide regions. For cyclohexane UA model,

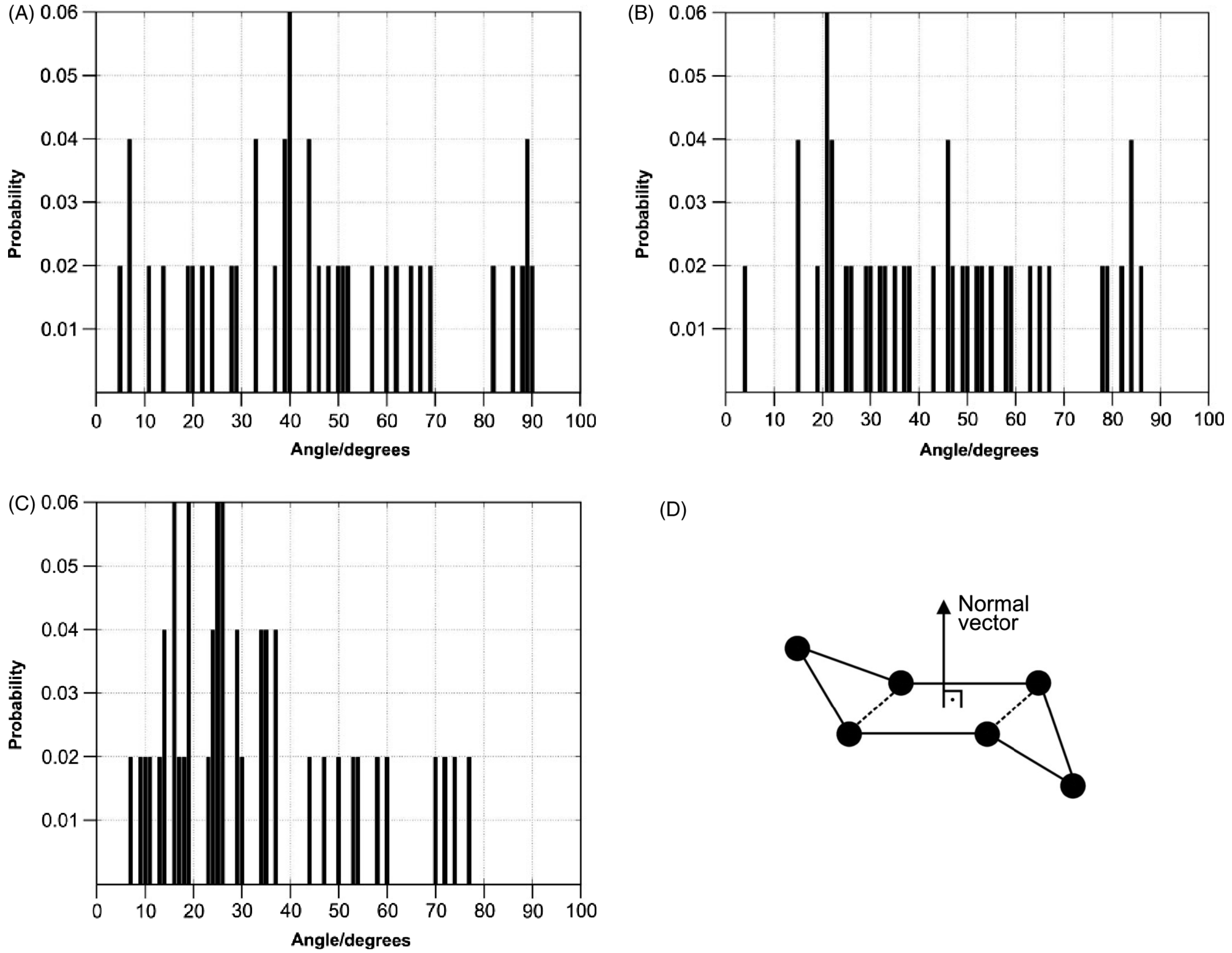

Figure 8. Probabilities for normal angle between the plane of the aromatic ring and the crystallographic *c*-axis. (A) Cyclohexane AA model; (B) cyclohexane UA model; (C) cyclohexane AUA model; and (D) representation of the normal vector.

the adsorption sites disappear entirely. The cyclohexane AUA model presents an intermediate pattern between the two other models.

3.3 *o*-Xylene

3.3.1 Adsorption isotherms. The adsorption isotherms of *o*-xylene in $AlPO_4$-5 were simulated at 30°C and compared with experimental data of Chiang *et al.* [25]. Figure 11 presents the simulated and the experimental isotherms. The AUA force field shows higher values for the adsorbed phase concentrations (about 9%) when compared to the AA model at all loadings. As for cyclohexane, *o*-xylene adsorbed phase concentration values for the AA model are initially larger than the experimental data. The same real sieve imperfections observation can be also done here.

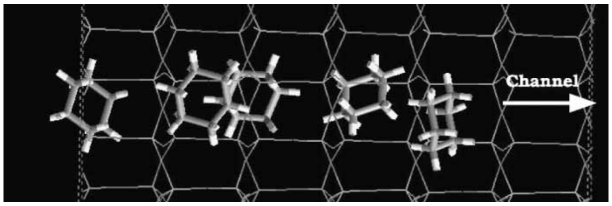

Figure 9. Typical pore side view of the cyclohexane molecules adsorbed in $AlPO_4$-5 at 30°C, using cyclohexane AA model, showing the asymmetric molecular pattern.

The low coverage adsorption heat for *o*-xylene AA and AUA models were calculated as 18.0 and 18.8 kcal/mol, respectively. A reported experimental low coverage adsorption heat is 17.6 kcal/mol [25]. The *o*-xylene AA low coverage adsorption heat was fitted to the experimental data from Chiang *et al.* [25], so the *o*-xylene AUA low coverage adsorption heat was a good approximation since this force field was fitted to butane in silicalite [37].

3.3.2 Structural analysis: molecular positioning and adsorption sites. In *o*-xylene, we cannot find variations in molecular positioning or adsorption sites (figures 12 and 13). The angles formed by the normal vector to the benzene ring concentrate on a range of low values corresponding to the positioning face-to-face of the benzene as it was previously proposed [25] based on

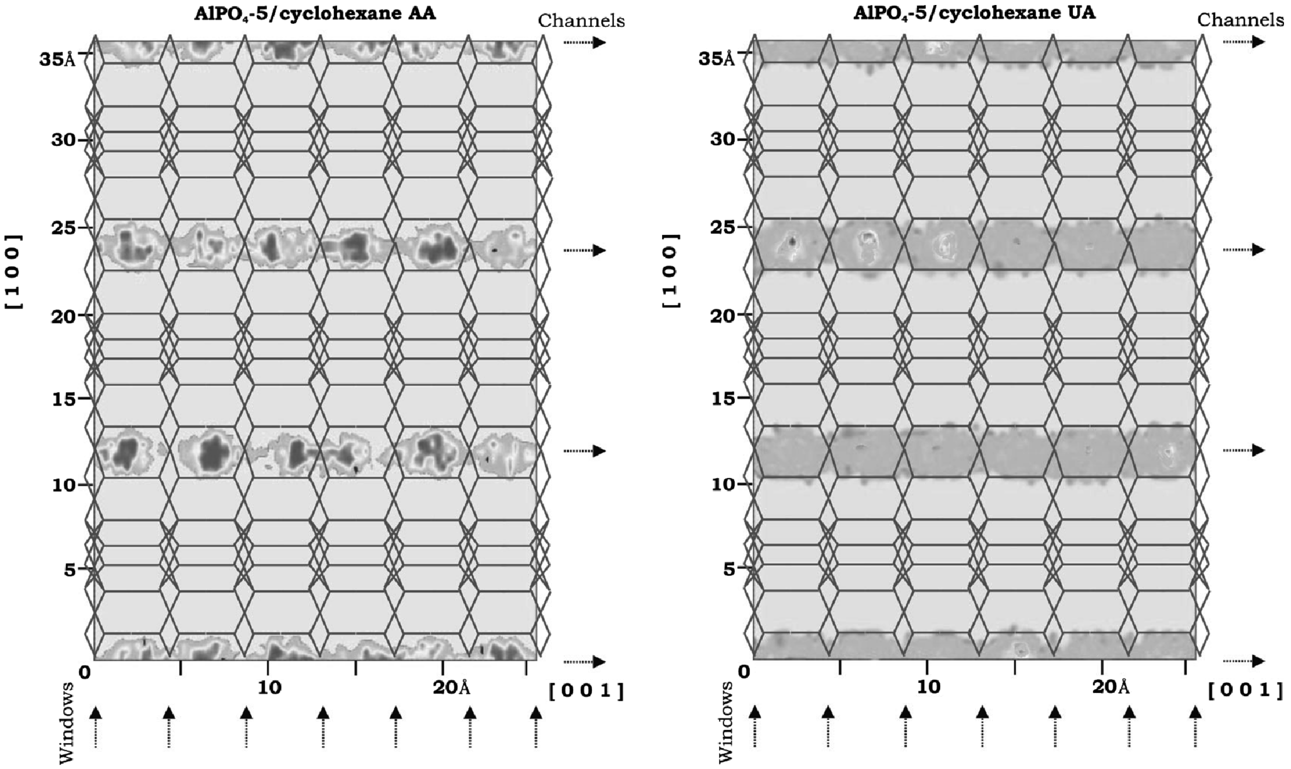

Figure 10. View of the 3 × 3 × 3 simulation cell in $AlPO_4$-5 for cyclohexane AA (left) and cyclohexane UA (right) with respective statistics of mass centres location of the success moves during simulation. Projection down plane (0 1 0). Dark areas are of high mass centres occurrence. Note the absence of adsorption sites in the cyclohexane UA model (right). The cyclohexane AUA model yields an intermediate pattern between AA and UA results.

experimental data. Both force fields reproduce well this positioning. The adsorption sites are preferentially located in the wide regions and again the two force fields agree with this pattern.

A possible explanation of these results may be related to a critical geometric condition identified by Yashonath and co-workers [1,35,45,46], in molecular dynamics studies for diffusion anomalies in molecular sieves, denominated levitation effect. In this condition, the net forces on the guest due to the host is at a minimum, the levitation ratio (γ) is close to unity and we have a weakly bound guest that can be easily moved from its equilibrium position. In those studies, for several different molecules, systems with γ between 0.95 and 1.05 would present levitation effect. On the other hand, systems with γ above 1.13 would definitely not present the levitation effect.

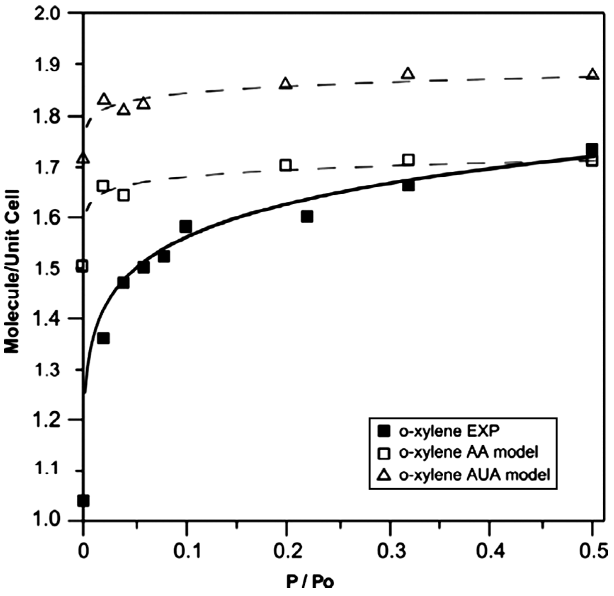

Figure 11. Adsorption isotherms of *o*-xylene in $AlPO_4$-5 at 30°C ($P_o = 1.18\,\mathrm{kPa}$). Our simulation (dashed lines and open symbols); experimental data [25] (filled lines and symbols).

So benzene and cyclohexane, that showed results that were more affected by the choice of force field, would have such dimensions that would result in levitation ratios (γ) close to unity. On the other hand, *o*-xylene, which is only slightly affected by the choice of the force field, should have levitation ratio different from unity.

To test this hypothesis, we used the equation proposed by Ghorai *et al.* [45] for the levitation ratio:

$$\gamma = \frac{2^{7/6}\sigma_{\mathrm{gh}} + l}{\sigma_{\mathrm{w}}}$$

where σ_{gh} is the hydrogen–oxygen (guest–host) interaction parameter and σ_{w} is the window diameter defined as the centre to centre distance between diagonal oxygen atoms of the channel. In their study, l was the end-to-end distance between the atomic centres of the linear guest. To adapt to cyclic molecules, we defined l as the LJ kinetic diameter of the molecules.

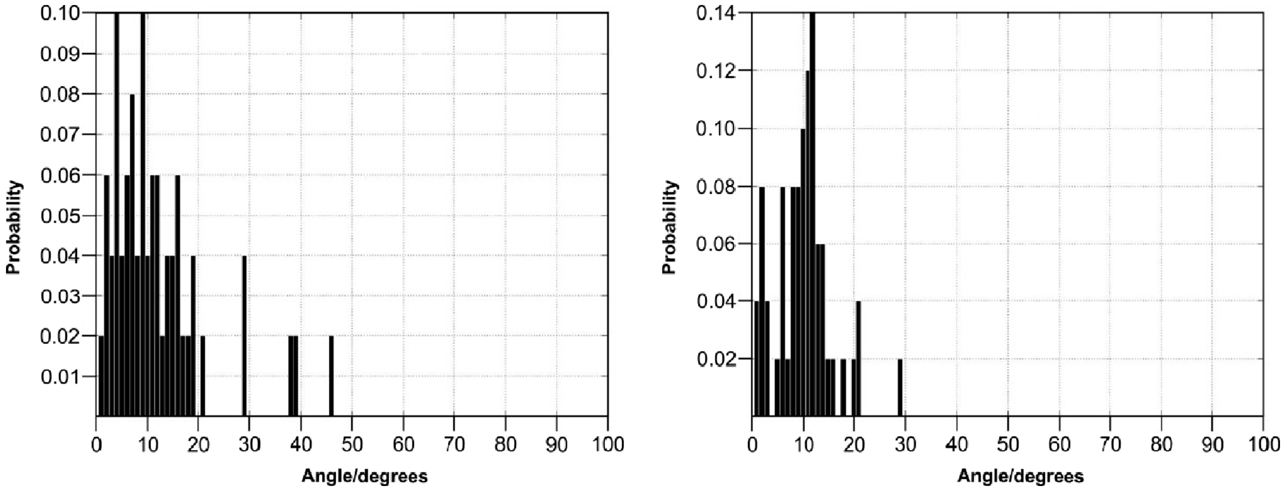

Figure 12. Probabilities for normal angle between the plane of the aromatic ring and the crystallographic *c*-axis. Left, *o*-xylene AA model and right, *o*-xylene AUA model.

In table 4, we show the values of the calculated parameters for $AlPO_4$-5 and the respective adsorbate molecules from our AA model data. We observe that the molecules of benzene and cyclohexane present levitation ratio values near 1.0. For *o*-xylene, however, the value of γ is 1.19, confirming our initial hypothesis.

Other evidences that support this reasoning can be extracted from the adsorption studies in two different limits: 1, smaller molecules such as methane in $AlPO_4$-5; and 2, *o*-xylene in aluminophosphate molecular sieves with diameters larger than $AlPO_4$-5 such as $AlPO_4$-8. We expect that small molecules do not alter their positioning (levitation ratios different from one) and that the *o*-xylene molecules, when in a larger sieve, would have levitation ratios approaching 1 resulting in positioning variations.

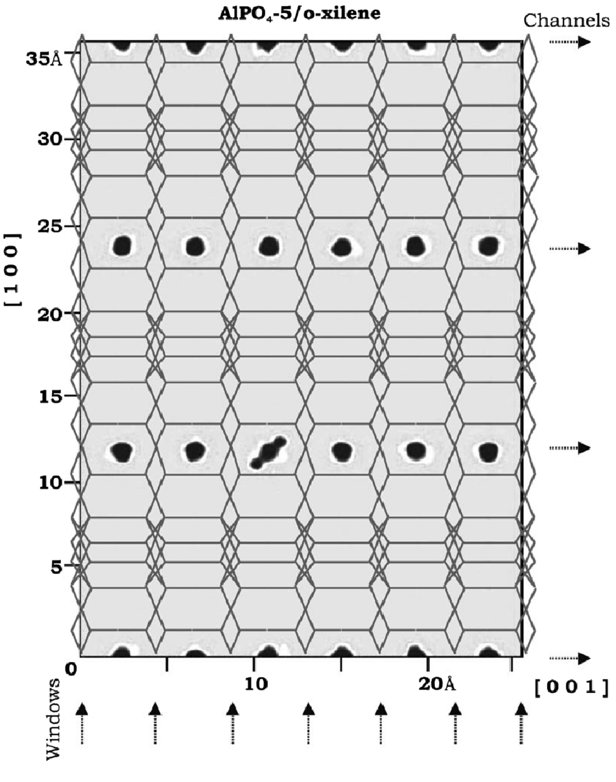

Figure 13. View of the 3 × 3 × 3 simulation cell of $AlPO_4$-5 and *o*-xylene with respective statistics of mass centres location of the success moves during simulation. Projection down plane (0 1 0). Dark areas are of high mass centres occurrence. Both models seem very similar.

Boutin *et al.* [42] and Maris *et al.* [49] in their studies of methane adsorption in $AlPO_4$-5 tested several AA and UA force fields. In these studies, despite the variations in the adsorption isotherm results, the methane molecules positioning stay the same. The adsorbed molecules are evenly located at *c*/4 and 3*c*/4 positions. For *o*-xylene in $AlPO_4$-8, we have found significant variations in the positioning of the molecules in a recent study [16].

4. Conclusions

We have shown that molecular positioning and adsorption sites of cyclic molecules vary among the several force fields tested. Benzene molecules have their face-to-face and parallel positioning changed while their adsorption sites are maintained. Cyclohexane molecules do not change their positioning but their adsorption sites lose the original configuration depending on the force field used. For *o*-xylene molecules, neither molecular positioning or adsorption sites have changed.

The simulation revealed a new positioning for the benzene (parallel) different from that proposed in the literature (face-to-face). The positioning of upright stacking of cyclohexane was not confirmed; the molecule does not have preferential positioning and assumes angular configurations in the whole spectrum.

Table 4. Dimensions and levitation ratios for benzene, cyclohexane and *o*-xylene (from the AA model data).

	σ_w (Å)	σ_{gh} (Å)	l (Å)	γ
Benzene	11.2	2.71	5.85 [47]	1.06
Cyclohexane	11.2	2.71	6.00 [47]	1.07
o-xylene	11.2	2.71	7.27 [48]	1.19

The new AUA force field proposed by Contreras-Camacho [27,28] showed a reasonable transferability in the aluminophosphate molecular sieves with results always close to the AA models fitted for aluminophosphates.

The fact that the different force fields did not result in alterations for positioning and adsorption sites of *o*-xylene in $AlPO_4$-5 can be related to the critical geometric condition denominated levitation effect. In our evaluation, benzene and cyclohexane presented levitation ratio values close to unity while *o*-xylene showed larger values. This is, to our knowledge, the first time that a MC molecular simulation study shows an evidence of the levitation effect that had been proposed from molecular dynamics studies for diffusion anomalies in molecular sieves.

Acknowledgements

The authors wish to acknowledge financial support for this study from CAPES, CNPq and FINEP/CTPETRO.

References

[1] S. Yashonath, P. Santikaryt. Diffusion of sorbates in zeolites Y and A: novel dependence on sorbate size and strength of sorbate–zeolite interaction. *J. Phys. Chem.*, **98**, 6368 (1994).

[2] A.H. Fuchs, A.K. Cheetham. Adsorption of guest molecules in zeolitic materials: computational aspects. *J. Phys. Chem. B*, **105**, 7375 (2001).

[3] A.V. Kiselev, P.Q. Du. Molecular statistical calculation of the thermodynamic adsorption characteristics of zeolites using the atom–atom aproximation. *J. Chem. Soc. Faraday Trans. II*, **77**, 17 (1981).

[4] A.V. Kiselev, A.A. Lopatkin, A.A. Shulga. Molecular statistical calculation of gas adsorption by silicalite. *Zeolites*, **5**, 261 (1985).

[5] B. Smit, J.I. Siepmann. Computer simulations of the energetics and siting of *n*-alkanes in zeolites. *J. Phys. Chem.*, **98**, 8442 (1994).

[6] J.I. Siepmann, S. Karaborni, B. Smit. Simulating the critical behaviour of complex fluids. *Nature*, **365**, 330 (1993).

[7] M.D. Macedonia, E.J. Maginn. A biased grand canonical Monte Carlo method for simulating adsorption using all-atom and branched united atom models. *Mol. Phys.*, **96**, 1375 (1999).

[8] S. Toxvaerd. Molecular dynamics calculation of the equation of state of alkanes. *J. Chem. Phys.*, **93**, 4290 (1990).

[9] R.J-M. Pellenq, B. Tavitian, D. Espinat, A.H. Fuchs. Grand canonical Monte Carlo simulations of adsorption of polar and nonpolar molecules in NaY zeolite. *Langmuir*, **12**, 4768 (1996).

[10] T. Kitagawa, T. Tsunekawa, K. Iwayama. Experimental and molecular simulation studies of adsorption and diffusion of cyclic hydrocarbons in silicalite-1. *Microporous Mater.*, **7**, 227 (1996).

[11] V. Lachet, A. Boutin, B. Tavitian, A.H. Fuchs. Molecular simulation of *p*-xylene and *m*-xylene adsorption in Y zeolites. Single components and binary mixtures study. *Langmuir*, **15**, 8678 (1999).

[12] V. Lachet, A. Boutin, B. Tavitian, A.H. Fuchs. Computational study of *p*-xylene/*m*-xylene mixtures adsorbed in NaY zeolite. *J. Phys. Chem. B*, **102**, 9224 (1998).

[13] R.Q. Snurr, A.T. Bell, D.N. Theodorou. Prediction of adsorption of aromatic hydrocarbons from grand canonical Monte Carlo simulations with biased insertions. *J. Phys. Chem.*, **97**, 13742 (1993).

[14] R.Q. Snurr, A.T. Bell, D.N. Theodorou. Molecular simulations of low occupancy adsorption of aromatics in silicalite. *Proceedings from the Ninth International Zeolite Conference*, Vol. II, pp. 71 (1993).

[15] S.M.P. Lucena, J.A.F.R. Pereira, C.L. Cavalcante Jr. Structural analysis and adsorption sites of xylenes in $AlPO_4$-5 and $AlPO_4$-11 using molecular simulation. *Microporous Mesoporous Mater.*, **88**, 135 (2006).

[16] S.M.P. Lucena, J.A.F.R. Pereira, C.L. Cavalcante Jr. *Ortho*-selectivity in aluminophosphate molecular sieves: a molecular simulation study. *Adsorption*, **12**, 425 (2006).

[17] P. Demontis, S. Yashonath, M.L. Klein. Localization and mobility of benzene in sodium-Y zeolite by molecular dynamics calculations. *J. Phys. Chem.*, **93**, 5016 (1989).

[18] S.M. Auerbach, L.M. Bull, N.J. Henson, H.I. Metiu, A.K. Cheetham. Behavior of Benzene in Na-X and Na-Y Zeolites: comparative study by 2H NMR and molecular mechanics. *J. Phys. Chem.*, **100**, 5923 (1996).

[19] H. Klein, H. Fuess, G. Schrimpf. Mobility of aromatic molecules in zeolite NaY by molecular dynamics simulation. *J. Phys. Chem.*, **100**, 11101 (1996).

[20] L.A. Clark, R.Q. Snurr. Adsorption isotherm sensitivity to small changes in zeolite structure. *Chem. Phys. Lett.*, **308**, 155 (1999).

[21] J.P. Fox, V. Rooy, S.P. Bates. Simulating the adsorption of linear, branched and cyclic alkanes in silicalite-1 and AlPO4-5. *Microporous Mesoporous Mater.*, **69**, 9 (2004).

[22] A. Gupta, L.A. Clark, R.Q. Snurr. Grand canonical Monte Carlo simulations of nonrigid molecules: siting and segregation in silicalite zeolite. *Langmuir*, **16**, 3910 (2000).

[23] M. Schenk, B. Smit, T.L.M. Maesen, T.J.H. Vlugt. Molecular simulations of the adsorption of cycloalkanes in MFI-type silica. *Phys. Chem. Chem. Phys.*, **7**, 2622 (2005).

[24] B.L. Newalkar, R.V. Jasra, V. Kamath, S.G.T. Bhat. Sorption of C6 alkanes in aluminophosphate molecular sieve, AlPO4-5. *Adsorption*, **5**, 345 (1999).

[25] A.S.T. Chiang, C.K. Lee, Z.H. Chang. Adsorption and diffusion of aromatics in AlPO4-5. *Zeolites*, **11**, 380 (1991).

[26] P. Ungerer, C. Beauvais, J. Delhommelle, A. Boutin, B. Rousseau, A.H. Fuchs. Optimization of the anisotropic united atoms intermolecular potential for *n*-alkanes. *J. Chem. Phys.*, **112**, 5499 (2000).

[27] R.O. Contreras-Camacho, P. Ungerer, A. Boutin, A.D. Mackie. Optimized intermolecular potential for aromatic hydrocarbons based on anisotropic united atoms. 1. Benzene. *J. Phys. Chem. B*, **108**, 14109 (2004).

[28] R.O. Contreras-Camacho, P. Ungerer, M.G. Ahunbay, V. Lachet, J. Perez-Pellitero, A.D. Mackie. Optimized intermolecular potential for aromatic hydrocarbons based on anisotropic united atoms. 2. Alkylbenzenes and styrene. *J. Phys. Chem. B*, **108**, 14115 (2004).

[29] E. Bourasseau, P. Ungerer, A. Boutin. Prediction of equilibrium properties of cyclic alkanes by Monte Carlo simulations new anisotropic united atoms intermolecular potentials new transfer bias method. *J. Phys. Chem. B*, **106**, 5483 (2002).

[30] J.M. Bennet, J.P. Cohen, E.M. Flanigen, J.J. Pluth, J.V. Smith. Crystal structure of tetrapropylammonium hydroxide–aluminum phosphate. *ACS Symp. Ser.*, **218**(5), 109 (1983).

[31] W.L. Jorgensen, D.L. Severance. Aromatic–aromatic interactions: free energy profiles for the benzene dimer in water, chloroform, and liquid benzene. *J. Am. Chem. Soc.*, **112**, 4768 (1990).

[32] S.L. Mayo, B.D. Olafson, W.A. Goddard. DREIDING: a generic force field for molecular simulations. *J. Phys. Chem.*, **94**, 8897 (1990).

[33] A.L. Rodriguez, C. Vega, J.J. Freire, S. Lago. Potential parameters of methyl and methylene obtained from second virial coefficients of *n*-alkanes. *Mol. Phys.*, **73**(3), 691 (1991).

[34] W.L. Jorgensen, E.R. Laird, T.B. Nguyen, J. Tirado-Rives. Monte Carlo simulations of pure liquid substituted benzenes with OPLS potential functions. *J. Comp. Chem.*, **14**, 206 (1993).

[35] S.Y. Bhide, S. Yashonath. Structure and dynamics of benzene in one-dimensional channels. *J. Phys. Chem. B*, **104**, 11977 (2000).

[36] J. Jänchen, H. Stach, L. Uytterhoeven, W.J. Mortier. Influence of the framework density and effective electronegativity of silica and aluminophosphate molecular sieves on the heat of adsorption od nonpolar molecules. *J. Phys. Chem.*, **100**, 12489 (1996).

[37] P. Pascual, P. Ungerer, B. Tavitian, P. Pernot, A. Boutin. Development of a transferable guest–host force field for adsorption of hydrocarbons in zeolites. I. Reinvestigation of alkanes adsorption in silicalite by grand canonical Monte Carlo simulation. *Phys. Chem. Chem. Phys.*, **5**, 3684 (2003).

[38] P. Pascual, H. Kirsch, A. Boutin, J-L. Paillaud, M. Soulard, B. Tavitian, D. Faye, A.H. Fuchs. Adsorption of various hydrocarbons in siliceous zeolites: a molecular simulation study. *Adsorption*, **11**, 379 (2005).

[39] N. Karasawa, W.A. Goddard III. Acceleration of convergence for lattice sums. *J. Phys. Chem.*, **93**, 7320 (1989).

[40] D. Frenkel, B. Smit. *Understanding Molecular Simulation*, Academic Press, New York (2002).

[41] G. Vitale, C.F. Mellot, A.K. Cheetham. Localization of adsorbed cyclohexane in the acid form of zeolite Y. A powder neutron diffraction and computational study. *J. Phys. Chem. B*, **101**, 9886 (1997).

[42] A.P. Boutin, J.-M. Roland, D. Nicholson. Molecular simulation of the stepped adsorption isotherm of methane in $AlPO_4$-5. *Chem. Phys. Lett.*, **219**, 484 (1994).

[43] Sorption, invoked from Cerius2 v. 4.6, Accelrys Inc., San Diego (2001).

[44] S.B. McCullen, P.T. Reischman, D.H. Olson. Hexane and benzene adsorption by aluminophosphates and SSZ-24: the effect of pore size and molecular sieve composition. *Zeolites*, **13**, 640 (1993).

[45] P.Kr. Ghorai, S. Yashonath, P. Demontis, G.B. Suffritti. Diffusion anomaly as a function of molecular length of linear molecules: levitation effect. *J. Am. Chem. Soc.*, **125**, 7116 (2003).

[46] S. Bandyopadhyay, S. Yashonath. Diffusion anomaly in silicalite and VPI-5 from molecular dynamics simulations. *J. Phys. Chem.*, **99**, 4286 (1995).

[47] D.W. Breck. *Zeolite Molecular Sieve*, John Wiley & sons, p. 636 (1974).

[48] C.E. Webster, R.S. Drago, M.C. Zerner. Molecular dimensions for adsorptives. *J. Am. Chem. Soc.*, **120**, 5509 (1998).

[49] T. Maris, T.J.H. Vlugt, B. Smit. Simulation of alkane adsorption in the aluminophosphate molecular sieve $AlPO_4$-5. *J. Phys. Chem. B*, **102**, 7183 (1998).